

Improving Accuracy and Efficiency of Start-up Cost Formulations in MIP Unit Commitment by Modeling Power Plant Temperatures

Matthias Silbernagl, Matthias Huber, and René Brandenberg

Abstract—This paper presents an improved mixed-integer model for the Thermal Unit Commitment Problem. By introducing new variables for the temperature of each thermal unit, the off-time-dependent start-up costs are modeled accurately while using fewer inequalities than state-of-the-art formulations. This new approach significantly improves computational efficiency, even compared to existing formulations which only roughly approximate start-up costs. Our findings were validated on real-world test cases using CPLEX and Xpress.

Index Terms—Thermal Unit Commitment, Mixed Integer Programming, Start-up Costs, Power Plant Temperatures, Residual Temperature Inequalities, Integration of Renewables

NOMENCLATURE

Indices and Sets

| | |
|---------------------|--|
| $t \in \mathcal{T}$ | Time periods, $\mathcal{T} = [1 .. T]$ |
| $i \in \mathcal{I}$ | Generating units |
| $l \in \mathbb{N}$ | Look-back time |

Parameters

| | |
|------------------|---|
| L^t | Electricity demand [MW] |
| P_i^{\max} | Maximum power output [MW] |
| P_i^{\min} | Minimum power output [MW] |
| RU_i | Maximum ramp up speed [MW/period] |
| RD_i | Maximum ramp down speed [MW/period] |
| SU_i | Maximum ramp up at start-up [MW] |
| SD_i | Maximum ramp down at shutdown [MW] |
| B_i | Variable production cost [$\text{cost}/\text{MWperiod}$] |
| A_i | Fixed cost while online [$\text{cost}/\text{period}$] |
| K_i^l | Start-up cost after l offline periods [cost] |
| K_{tol} | Start-up cost approximation tolerance (relative) |
| λ_i | Heat-loss coefficient, $\lambda_i \in (0, 1)$ [$1/\text{period}$] |
| V_i | Variable start-up cost [cost] |
| F_i | Fixed start-up cost [cost] |
| PD_i | Offline periods prior to first period [period] |

Variables

| | |
|-------------------|--|
| v_i^t | State of power plant, $v_i^t \in \{0, 1\}$ |
| p_i^t | Power output [MW] |
| temp_i^t | Temperature, normalized to $[0, 1]$ |
| h_i^t | Heating, normalized to $[0, 1]$ |
| z_i^t | Start-up status, $z_i^t \in \{0, 1\}$ |

Variables (cont.)

| | |
|----------|-------------------------|
| cp_i^t | Production costs [cost] |
| cu_i^t | Start-up costs [cost] |

I. INTRODUCTION

RENEWABLE power sources are being introduced in many of the world's power systems [1]. The intermittent nature of the power production from these sources, especially of wind and solar, is leading to a higher number of start-ups of conventional thermal power plants [2], [3]. Consequently, the percentage of costs caused by start-ups is increasing, and accurate start-up cost models are gaining importance.

Operational planning of power systems includes the scheduling of power generating units, which is known as the Unit Commitment (UC) problem [4]. Finding cost-optimal solutions to this problem has been an active field of research since almost the beginning of electrification [5], and a wide variety of optimization approaches have been applied [6], [7].

A prevalent employed approach is Mixed Integer Programming (MIP) by Branch&Cut, which is known for simultaneously producing a series of improving solutions and reducing their worst-case optimality gap, ultimately leading to an optimal solution. Its main drawbacks are the restricted modeling flexibility and the high computational effort. Both issues have been mitigated by new UC formulations, faster solvers, and greater computational power; still, further progress is vital. This paper contributes by improving the formulation of the start-up costs.

A. Literature Review

We base our work on the widely used MIP formulation given in [8]. Since its publication in 2006, numerous advancements have been published; we restrict ourselves to mentioning only those with a focus similar to our work. In [9], an application to the self scheduling problem with a more accurate start-up process is presented, introducing start-up types. Even when disregarding the start-up process, in comparison with [8], these start-up types lead to tighter formulations (as proved in [10]).

Tighter UC formulations have been of interest in general. In [11], the minimal up- and down-time constraints are considered. It is proved that the feasible operational schedules can be described by $\mathcal{O}(2^{|\mathcal{T}|}|\mathcal{I}|)$ inequalities. By using start-up and shutdown status variables, [12] characterizes the same feasible set with only $\mathcal{O}(|\mathcal{I}||\mathcal{T}|)$ inequalities—a prime example of how

representations of polytopes may be simplified by introducing additional variables.

The quadratic production costs have commonly been modeled by piece-wise linear approximations. [13] presents tight valid inequalities for these costs, enabling an iterative approximation scheme. A similar approximation scheme with different valid inequalities is given in [14]. Finally, in [15], valid inequalities for the ramping process are presented, leading to considerably faster solution times.

B. Contribution and Paper Organization

The focus of this paper is a novel approach to modeling the start-up costs. After a short recapitulation of the prevalent state-of-the-art formulations in Section II, our contributions are introduced in the following order.

Section III-A introduces a simple modification of the start-up cost model as presented by [16], which reduces the integrality gap of the model.

Section III-B considers an approximation algorithm previously published in [17]. This algorithm, given an approximation tolerance, computes an approximation of the start-up cost function with a minimum number of steps. While current UC models [8]–[10], [15], [16], [18] allow the discretization of the start-up cost function using an arbitrary number of steps, the problem of selecting these steps is not addressed. For numerical experiments, typically a fixed number of steps is apparently chosen by expert guess (hot/cold steps in [15], hot/warm/cold steps in [8]–[10], five steps in [18]). However, the number of steps needed to bound the maximal approximation error depends on the ratio of variable to fixed start-up costs of each individual unit. Our algorithm overcomes this limitation by optimally selecting steps for each unit, leading to a fewer number of steps or a lower approximation error (or both).

Section IV examines the derivation of the commonly used start-up cost function from a simple physical model. This motivates the formulation presented in the following section and serves as a satisfying interpretation.

Section V presents the new approach which explicitly models the cooling behavior of units during the offline time by introducing temperature variables. After shutting down a unit, its temperature decays exponentially. At start-up, the lost thermal energy, which is proportional to the temperature loss, must be compensated for by burning additional fuel. By internalizing this physical process instead of encapsulating it in the start-up cost parameters K_i^l , this formulation is able to model exact start-up costs for arbitrarily long offline times. Moreover, it significantly improves computational performance compared to existing formulations by considerably reducing the integrality gap and the solution time of the linear relaxation.

Section VI further reduces the integrality gap of the new formulation by adding a class of inequalities, which we call *residual temperature inequalities (RTIs)*. These inequalities are added to the problem in a cutting plane approach, using a computationally efficient exact separation algorithm.

Section VII lists results of numerical experiments, which clearly show the advantages of the proposed approach.

The paper ends with a summary and an outlook on further research directions.

II. STATE OF THE ART

This section describes the basis of the two prevalent MIP models in recent publications: the approach of [8] with 1 binary variable per unit and period ("1-Bin") as well as the approach with 3 binaries ("3-Bin") according to [15], which proved to model start-up costs more efficiently [10].

A. Base Model

The goal of the UC problem is to fulfill the electricity demand L^t at minimal cost. The costs comprise two parts: production costs and start-up costs. Using the production costs cp_i^t and the start-up costs cu_i^t , the UC problem may be modeled as

$$\min \sum_{i \in \mathcal{I}, t \in \mathcal{T}} cp_i^t + cu_i^t \text{ s.t.} \quad (1)$$

$$\sum_{i \in \mathcal{I}} p_i^t = L^t \quad \forall t \in \mathcal{T}. \quad (2)$$

The start-up costs are discussed in Section II-B. The production costs are non-convex [19], [20], and approximated by a piece-wise linear function in [8]. As the focus of this paper lies on the start-up costs, we use the simpler production costs in [10], which depend linearly on the binary operational state v_i^t and the production p_i^t :

$$cp_i^t = A_i v_i^t + B_i p_i^t \quad \forall i \in \mathcal{I}, t \in \mathcal{T} \quad (3)$$

Generally used constraints of thermal power plants regard the minimal production P_i^{\min} , the maximal production P_i^{\max} , maximal up and down ramping speeds RU_i and RD_i as well as maximal ramping at start-up SU_i and shutdown SD_i . These constraints may be formulated as

$$p_i^t \leq p_i^{t-1} + RU_i v_i^{t-1} + SU_i (1 - v_i^{t-1}) - \min \{SU_i, P_i^{\min} + RU_i\} (1 - v_i^t) \quad \forall i \in \mathcal{I}, t \in [2 .. T], \quad (4)$$

$$p_i^t \geq p_i^{t-1} - RD_i v_i^t - SD_i (1 - v_i^t) + \min \{SD_i, P_i^{\min} + RD_i\} (1 - v_i^{t-1}) \quad \forall i \in \mathcal{I}, t \in [2 .. T], \quad (5)$$

$$p_i^t \leq P_i^{\max} v_i^{t+1} + SD_i (v_i^t - v_i^{t+1}) \quad \forall i \in \mathcal{I}, t \in [1 .. T-1]. \quad (6)$$

B. Start-up Costs

The start-up costs depend on the amount of time l that a unit has been offline before a start-up. For thermal units, they are typically modeled according to [21], [22] as

$$K_i^l = V_i (1 - e^{-\lambda_i l}) + F_i \quad \forall i \in \mathcal{I}, l \in \mathbb{N} \quad (7)$$

where F_i are the fixed start-up costs and V_i are the maximum variable start-up costs, such that the costs for a complete cold start are $V_i + F_i$. The fixed costs include labor costs as well as time-independent wear and tear costs. As the modeled time range is discretized into periods, only integer offline times $l \in \mathbb{N}$ may occur (cf. Fig. 1).

1) *Formulation with one binary variable (“1-Bin”)*: In the prevalent start-up cost model, the cost function is approximated by an increasing step function, i.e. a piece-wise constant, increasing function. This formulation has been used in numerous publications with a fixed number of steps, and was first generalized to an arbitrary number of steps in [16]:

$$cu_i^t \geq K_i^l \left(v_i^t - \sum_{n=1}^l v_i^{t-n} \right) \quad \forall i \in \mathcal{I}, t \in \mathcal{T}, l \in [1 \dots t-1]. \quad (8)$$

These inequalities properly model arbitrary increasing start-up cost functions.

Note that to incorporate the offline time PD_i preceding the modeled time range, in the case $l = t - 1$ the start-up costs $K_i^{t-1+PD_i}$ need to be used. We disregard this technicality for the sake of a simpler presentation.

2) *Formulation with three binary variables (“3-Bin”)*: The authors of [10] and [15] show that modeling the operational state with three sets of binary variables is computationally more efficient than the model with 1 binary described above. We therefore include this formulation in the numerical experiments, in an implementation equivalent to the model P1 in [10].

The two additional sets of binary variables used to describe the operational state are the start-up state z_i^t and the shutdown state w_i^t (c.f. [23]), which are modeled by the equation

$$z_i^t - w_i^t = v_i^t - v_i^{t-1} \quad \forall i \in \mathcal{I}, t \in \mathcal{T}. \quad (9)$$

The start-ups are classified into types according to their costs using the binary variables $\delta_i^t(l)$,

$$\sum_{\substack{l \in [1 \dots t-1] \\ K_i^l < K_i^{l+1}}} \delta_i^t(l) = z_i^t \quad \forall i \in \mathcal{I}, t \in \mathcal{T}, \quad (10)$$

such that $\delta_i^t(l) = 1$ if and only if unit i starts up in period t with cost K_i^l , i.e. if the start-up it is preceded by a shutdown and offline time of correct length,

$$\delta_i^t(l) \leq \sum_{\substack{n \in [1 \dots l] \\ K_i^n = K_i^l}} w_i^{t-n} \quad \forall i \in \mathcal{I}, t \in \mathcal{T}, \quad (11) \\ l \in [1 \dots t-1], K_i^l < K_i^{l+1}.$$

Instead of (8), the start-up costs are derived by

$$cu_i^t \geq \sum_{\substack{l \in [1 \dots t-1] \\ K_i^l < K_i^{l+1}}} K_i^l \delta_i^t(l) \quad \forall i \in \mathcal{I}, t \in \mathcal{T}. \quad (12)$$

III. IMPROVING THE 1-BIN AND 3-BIN FORMULATIONS

In this section, we present a modification of the constraints in (8) that tightens 1-Bin, and a method to control the approximation error of the time-dependent start-up costs in both 1-Bin and 3-Bin.

A. Tightening the 1-Bin Formulation

The inequalities (8) can be tightened by lessening the coefficients of the variables v_i^{t-n} ,

$$cu_i^t \geq K_i^l v_i^t - \sum_{n=1}^l (K_i^l - K_i^{n-1}) v_i^{t-n} \\ \forall i \in \mathcal{I}, t \in \mathcal{T}, l \in [1 \dots t-1]. \quad (13)$$

Each of these inequalities is trivially fulfilled if unit i is offline in period t , since then its right-hand side is non-positive. If unit i is online in period t , consider all $n \in [1 \dots l]$ with $v_i^{t-n} = 1$. If no such n exists, then both the start-up costs cu_i^t and the right-hand side of the inequality equal K_i^l . Otherwise, choose a minimal n with this property. Then, the start-up costs cu_i^t equal K_i^{n-1} , and the right-hand side is at most K_i^{n-1} . As these inequalities dominate those in (8), they still properly model the start-up costs.

The impact of the tightening on the integrality gap is depicted in Fig. 4 in Section VII.

B. Approximating the Time-dependent Start-up Cost

To keep computational efforts reasonable, the time-dependent start-up costs are often approximated either by a constant value (see e.g. [23], [24]) or by up to three steps, hot-, cold-, and possibly warm-start (see e.g. [25]). In the light of cool-down times of up to 120 hours for large thermal units [22], these approaches result in considerable approximation errors. This is addressed in [9], [16] and subsequently in [8], [10], [15], where an arbitrary number of steps is allowed. We present Alg. 1 from [17] which determines, given a certain approximation tolerance K_{tol} , how to choose these steps optimally.

When dropping the constraints in (8) or (13) for some l , one effectively models an approximation \tilde{K}_i^l of the start-up costs K_i^l . If the start-up costs K_i^l for some look-back times $l^* - 1$ and l^* are equal, then the constraints (8) for $l = l^* - 1$ dominate the constraints (8) for $l = l^*$. Unsurprisingly, the tightened constraints (13) for $l = l^*$ and $l = l^* - 1$ are equal in that case. Thus, redundant constraints in (8) and (13) are avoided by considering only look-back times l with $K_i^l > K_i^{l-1}$.

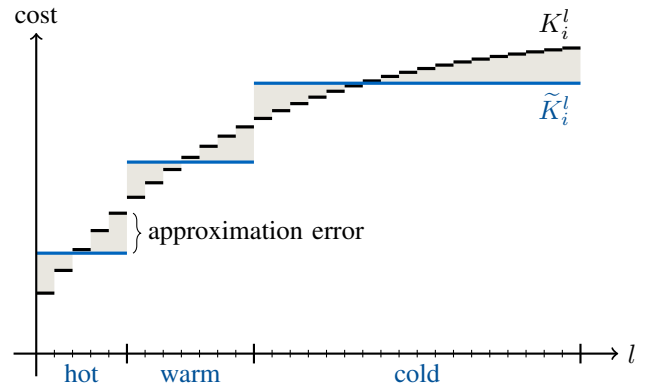


Fig. 1. Time-dependent start-up costs K_i^l and a three-step approximation \tilde{K}_i^l .

When solving MIPs, the goal typically is to reach a certain maximal relative optimality gap. Hence, the start-up cost approximation also needs to guarantee a maximal relative error,

$$\left| \tilde{K}_i^l - K_i^l \right| \leq K_{\text{tol}} \cdot K_i^l \quad \forall i \in \mathcal{I}, l \in [1 \dots T-1]. \quad (14)$$

Such an approximation with minimal number of different values can be found by iteratively grouping as many periods as possible into a single step, see Algorithm 1.

Algorithm 1: ApproximateStartupCosts

```

a ← 1
while a < T do
  b ← a
  while b ≤ T ∧  $\frac{K_i^{b+1} - K_i^a}{K_i^{b+1} + K_i^a} \leq K_{tol}$  do
    b ← b + 1
  for l ∈ [a .. b] do
     $\tilde{K}_i^l \leftarrow \frac{2K_i^a K_i^b}{K_i^b + K_i^a}$ 
  a ← b + 1

```

IV. START-UP COSTS OF THERMAL UNITS

The step-wise start-up cost model considered in the previous section is applicable for all increasing start-up cost functions. However, as is mentioned in the last section, the start-up cost function of a thermal unit is commonly (e.g. [21]) defined much more restrictively as

$$K_i^l = \underbrace{V_i(1 - e^{-\lambda_i l})}_{\text{variable cost}} + \underbrace{F_i}_{\text{fixed cost}} \quad \forall i \in \mathcal{I}, l \in \mathbb{N} \quad (15)$$

where l denotes the offline time. The constant costs are modeled using the start-up status variables z_i^t presented in [23] (without the shutdown status variables):

$$z_i^1 = \begin{cases} v_i^1 & \text{if } PD_i > 0, \\ 0 & \text{else,} \end{cases} \quad \forall i \in \mathcal{I} \quad (16)$$

$$z_i^t \geq v_i^t - v_i^{t-1} \quad \forall i \in \mathcal{I}, t \in [2 .. T], \quad (17)$$

$$z_i^t \in \{0, 1\} \quad \forall i \in \mathcal{I}, t \in \mathcal{T}. \quad (18)$$

The variable costs originate from the reheating process at start-up, where fuel needs to be burned and where the unit experiences thermal stress.

Here, the term $(1 - e^{-\lambda_i l})$ is proportional to the heat loss of the power plant incurred while offline, and models the exponential decay of the temperature,

$$\text{temp}_i(l) = e^{-\lambda_i l} \quad \forall i \in \mathcal{I}, l \in \mathbb{R}_{\geq 0}, \quad (19)$$

assuming the operational temperature is normalized to 1 and the environmental temperature is normalized to 0.

As shown in Fig. 2, (19) is discretized by a step-wise constant function with steps according to

$$\widehat{\text{temp}}_i^t := \begin{cases} 1 & \text{if } v_i^t = 1, \\ \text{temp}_i(l_i^t) = e^{-\lambda_i l_i^t} & \text{else,} \end{cases} \quad (20) \\ \forall i \in \mathcal{I}, t \in \mathcal{T},$$

where l_i^t denotes the number of periods that unit i is offline prior to period t .

The above nonlinear definition of $\widehat{\text{temp}}_i^t$ may be restated recursively as

$$\widehat{\text{temp}}_i^1 = \begin{cases} 1 & \text{if } v_i^1 = 1, \\ e^{-\lambda_i PD_i} & \text{else,} \end{cases} \quad \forall i \in \mathcal{I} \quad (21)$$

$$\widehat{\text{temp}}_i^t = \begin{cases} 1 & \text{if } v_i^{t-1} = 1 \text{ or } v_i^t = 1, \\ e^{-\lambda_i \widehat{\text{temp}}_i^{t-1}} & \text{else,} \end{cases} \quad (22) \\ \forall i \in \mathcal{I}, t \in [2 .. T].$$

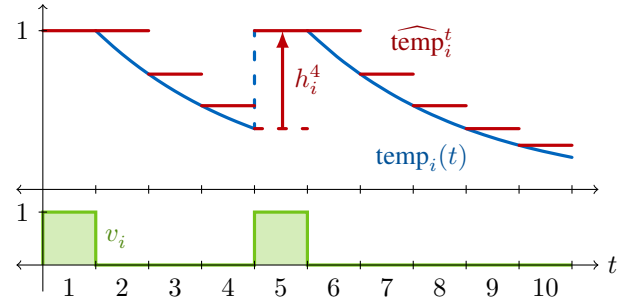


Fig. 2. Discretization of a unit's temperature function. Following the operational schedule, the unit exhibits the temperature function temp_i which is discretized to $\widehat{\text{temp}}_i$, with resulting heating h_i according to (26).

V. THE TEMPERATURE MODEL

In this section, we model the temperature loss derived in the last section by explicitly capturing the temperature of a unit as the new state variable temp_i^t and the amount of heating as the new variable h_i^t . Combined with the start-up status z_i^t (cf. IV), they are used to model the start-up cost function as defined in equation (7).

The new variables are continuous and non-negative,

$$\text{temp}_i^t \in \mathbb{R}_{\geq 0} \quad \forall i \in \mathcal{I}, t \in \mathcal{T}, \quad (23)$$

$$h_i^t \in \mathbb{R}_{\geq 0} \quad \forall i \in \mathcal{I}, t \in [0 .. T-1]. \quad (24)$$

The operational temperature is expressed as

$$v_i^t \leq \text{temp}_i^t \leq 1 \quad \forall i \in \mathcal{I}, t \in \mathcal{T}, \quad (25)$$

enforcing a temperature of exactly 1 during operation. The recursion in equations (21) and (22) is modeled as

$$\text{temp}_i^1 = e^{-\lambda_i PD_i} + h_i^0 \quad \forall i \in \mathcal{I}, \quad (26)$$

$$\text{temp}_i^t = e^{-\lambda_i} \text{temp}_i^{t-1} + (1 - e^{-\lambda_i}) v_i^{t-1} + h_i^{t-1} \quad (27) \\ \forall i \in \mathcal{I}, t \in [2 .. T],$$

which causes the temperature

- to decay exponentially while the unit is offline ($v_i^t = 0$),
- to stay constant at 1 while the unit is online ($v_i^t = 1$), and
- to rise by h_i^t if the unit is heating.

Finally, the start-up costs are modeled as

$$cu_i^t = V_i h_i^{t-1} + F_i z_i^t \quad \forall i \in \mathcal{I}, t \in \mathcal{T}. \quad (28)$$

We proceed by explaining the correctness of this model. It is easy to check that $z_i^t = 1$ exactly if there is a start-up in period t , and $z_i^t = 0$ otherwise. Thus, the constant part of the start-up costs is modeled correctly.

The temperature losses increase proportionally with $\text{temp}_i^t - v_i^t$. Thus, in a cost-minimal solution, heating is applied such that the temperature is minimal while fulfilling $\text{temp}_i^t \geq v_i^t$. This entails two consequences:

- 1) Heating is applied only in the period prior to each start-up. Earlier heating could be postponed until this period, thus saving heating costs.
- 2) The amount of heating is exactly such that the temperature reaches 1. Excessive heating could either be postponed until the period prior to the next start-up, or be avoided if there is no such start-up.

Therefore, in a cost-minimal solution, the temperature variables temp_i^t match the discretized temperatures $\widehat{\text{temp}}_i^t$ as given in equation (20), and the start-up costs cu_i^t equal 0 if unit i does not start-up in period t .

Given a cost-minimal solution, assume that unit i starts up in period t after l offline periods. By period $t-1$ the unit has cooled down for $l-1$ periods, and in period t , the temperature after start-up has to be 1 again,

$$\text{temp}_i^{t-1} \stackrel{(20)}{=} e^{-\lambda_i(l-1)} \quad \text{and} \quad \text{temp}_i^t \stackrel{(25)}{=} 1,$$

Thus, the needed heating, considering the further cooling during period $t-1$, matches the expected temperature loss,

$$\begin{aligned} h_i^{t-1} &\stackrel{(27)}{=} \text{temp}_i^t - e^{-\lambda_i} \text{temp}_i^{l-1} + (1 - e^{-\lambda_i}) \underbrace{v_i^{t-1}}_{=0} \\ &= 1 - e^{-\lambda_i}. \end{aligned}$$

This means, the variable part of the start-up costs is modeled correctly too, leading to $cu_i^t = K_i^l$.

While this model uses new additional variables, it reduces the number of constraints significantly in comparison to the step-wise start-up cost model. Fig. 4 suggests that the integrality gap of this model is typically smaller, and Fig. 5 evidences faster solution times for the linear relaxation. Both factors are crucial for the improved total solution times shown in Fig. 6.

However, one can construct example problems where the step-wise start-up cost model is tighter than the temperature model. This can be overcome by an additional class of constraints that are proposed in the next section.

VI. TIGHTENING THE TEMPERATURE MODEL

The linear relaxation of the temperature model can be improved by adding the inequalities

$$\text{temp}_i^t \geq \begin{cases} e^{-\lambda_i l} \text{temp}_i^{t-l} + (1 - e^{-\lambda_i l}) v_i^t & \text{if } l < t-1, \\ e^{-\lambda_i(l+PD_i)} + (1 - e^{-\lambda_i(l+PD_i)}) v_i^t & \text{else.} \end{cases} \quad \forall i \in \mathcal{I}, t \in \mathcal{T}, l \in [1 .. t-1] \quad (29)$$

which we call *residual temperature inequalities (RTIs)*. These inequalities improve the bounds in (25),

$$\text{temp}_i^t \geq v_i^t \quad \forall i \in \mathcal{I}, t \in \mathcal{T},$$

by considering the lowest possible temperature in each period. Over l offline periods, the temperature decays by a factor of $e^{-\lambda_i l}$, leading to

$$\text{temp}_i^t \geq \begin{cases} e^{-\lambda_i l} \text{temp}_i^{t-l} & \text{if } l \in [1 .. t-2], \\ e^{-\lambda_i l} \text{temp}_i^1 \geq e^{-\lambda_i(l+PD_i)} & \text{if } l = t-1. \end{cases}$$

Thus, the RTIs are fulfilled if $v_i^t = 0$. Secondly, $v_i^t = 1$ implies $\text{temp}_i^t = 1$, and by (25) the right hand side of an RTI never exceeds 1. Hence the RTIs are fulfilled for $v_i^t = 1$, too.

For a single unit i , the temperature model including RTIs completely describes the polyhedron of operational schedules v_i with corresponding summed start-up costs (see [26]). Thus, if the Unit Commitment MIP neither explicitly (e.g. min. downtime) nor implicitly (e.g. demand) prohibits any operational schedule $v_i \in \{0, 1\}^T$ of unit i , then the bound on the summed start-up costs of that unit can not be further improved.

Adding all RTIs to the formulation is not advisable, since it heavily increases the solution time of the linear relaxation. Thus, the inequalities are added as needed in a Branch&Cut approach, using the GAMS BCH facility [27] or the FICO Xpress Cut Manager Callback [28]. In both cases, the solver expects a user-supplied separation algorithm which, given a fractional solution to the linear relaxation, finds violated RTIs. We cite this separation algorithm and its main properties here, and refer to [26] for an in-depth discussion.

Since the separation algorithm processes each unit individually, only a single unit i is considered in the following. Out of the $\mathcal{O}(T^2)$ possible RTIs, it is sufficient to consider a certain subset of T inequalities depending on the current solution. If none of the inequalities in this subset are violated, then all RTIs are fulfilled by the current solution (see [26] for details).

To find the subset of relevant RTIs, a special binary tree on nodes numbered by \mathcal{T} is used, the so-called *Cartesian tree* on the sequence v_i^1, \dots, v_i^T . This data structure was first introduced in [29, Sect. 3.1] for two-dimensional points. We use the equivalent definition in [30, Sect. 3] for sequences, with the maximum value at the root. The needed Cartesian tree is represented by its root node η_1 and by vectors $\text{llink}, \text{rlink} \in (\mathcal{T} \cup \{\emptyset\})^T$ with $\text{llink}(t)$ defined as

- $\text{llink}(t) = \emptyset$ if node t has no left child,
- $\text{llink}(t) = l$ if node l is the left child of node t ,

and $\text{rlink}(t)$ defined equivalently for the right child of node t .

The relevant RTIs are checked by the following depth-first search routine on the Cartesian tree for v_i , which is started with $\text{SeparateRec}(\eta_1, \eta_1 - 1)$.

Function SeparateRec(node t , look-back time l)

```

if  $t \neq \emptyset$  then
  // Check RTI in current node  $t$ 
  if  $l = t - 1$  then
    | check  $\text{temp}_i^{t-l} \geq e^{-\lambda_i(l+PD_i)} + (1 - e^{-\lambda_i(l+PD_i)}) v_i^t$ 
  else
    | check  $\text{temp}_i^t \geq e^{-\lambda_i l} \text{temp}_i^{t-l} + (1 - e^{-\lambda_i l}) v_i^t$ 
  // Check RTIs in left/right subtree
  SeparateRec (llink( $t$ ),  $l - (t - \text{llink}(t))$ )
  SeparateRec (rlink( $t$ ),  $\text{rlink}(t) - t - 1$ )

```

SeparateRec visits each node exactly once, needing a running time of $\mathcal{O}(1)$ at each node, and thus possesses a complexity of $\mathcal{O}(T)$. Since the Cartesian tree may also be constructed in $\mathcal{O}(T)$ [30], the total running time of the separation over all units is $\mathcal{O}(|\mathcal{I}|T)$.

In our experiments we found it favorable to add multiple RTIs in each iteration of the cutting plane approach. To this end, the algorithm accumulates all violated RTIs of all units and selects a subset thereof for inclusion. The proposed heuristic selection algorithm starts with rating each RTI with

$$\text{rating} := \begin{cases} V_i \cdot \max\{0, \text{violation} - h_i^t\} & \text{if } t < T, \\ V_i \cdot \text{violation} & \text{else,} \end{cases} \quad (30)$$

where i and t denote the parameters of the RTI and “violation” denotes the amount by which the RTI is violated (right-hand side $- \text{temp}_i^t$).

The algorithm then selects a subset of RTI with maximal total rating such that

- at most M_i RTIs are selected per unit and
- at most M RTIs are selected in total.

In the conducted experiments, the constants $M_i := 0.15|\mathcal{T}|$ and $M := 0.5|\mathcal{I}|$ performed best.

To facilitate a straight-forward implementation of the separation algorithm, we cite the construction algorithm for Cartesian trees from [30, p. 138]. This algorithm starts with the trivial Cartesian tree for the one-dimensional vector (v_i^1) , and in each step $t \in [2 .. T]$ adds a node representing v_i^t at the appropriate spot on the “right shoulder” of the tree:

Function FindCartesianTree($v \in [0, 1]^T$)

```

// Initialize tree on  $(v_i^1)$ 
for  $t = 1, \dots, T$  do
  | llink( $t$ )  $\leftarrow \emptyset$ , rlink( $t$ )  $\leftarrow \emptyset$ 
 $\eta_1 \leftarrow 1$ ,  $R \leftarrow 1$ 
// Update tree to  $(v_i^1, \dots, v_i^t)$ 
for  $t = 2, \dots, T$  do
  | if  $v_i^{\eta_1} \leq v_i^t$  then // Insert as root
  |   | llink( $t$ )  $\leftarrow \eta_1$ 
  |   |  $\eta_1 \leftarrow t$ ,  $R \leftarrow 1$ 
  | else
  |   // Insert on right shoulder
  |   while  $v_i^{\eta_R} \leq v_i^t$  do
  |     |  $R \leftarrow R - 1$ 
  |     | llink( $t$ )  $\leftarrow$  rlink( $\eta_R$ )
  |     | rlink( $\eta_R$ )  $\leftarrow t$ 
  |     |  $\eta_{R+1} \leftarrow t$ ,  $R \leftarrow R + 1$ 

```

VII. NUMERICAL EXAMPLES

This section presents results from numerical examples which show the benefits of our modeling approach. After introducing the modeling setup¹, its reduced integrality gap and the increased computational performance of its linear relaxation are highlighted. These advantages lead to an overall faster optimization procedure and enable larger models to be solved.

A. Scenarios

The raising requirements for fossil-fuel power plants, which include a more volatile residual load, result in more start-ups and hence in a higher ratio of start-up to operational costs [2]. We expect the higher percentage of start-up costs to result in higher solution times and to increase the advantages of our approach. In order to show the impact of a more volatile residual load, two separate scenarios for 2014 and 2025 are considered for the numerical experiments.

We decided against using the power plant fleet proposed in [8] for two reasons:

- Due to advancements in computational performance, this dataset became too small for a meaningful comparison.

¹The complete dataset for these scenarios is included with this article on arXiv.

Previous publications (e.g. [10], [15]) remedy this by replicating its units multiple times. This however does not reflect the diversity of a real power system and introduces artificial symmetries which makes them harder to solve than usual [10].

- In [8], the start-up cost function is approximated by a step function with two steps (hot/cold), and an approximation error K_{tol} of at least 33%. As motivated in the introduction, more accurate start-up cost functions are necessary.

Instead, we use power plant data based on the German power system of 2014 as published by the German Federal Network Agency in [31], comprising 228 individually controlled power plants. This data is augmented by assumptions regarding the power plant parameters as shown in Table I, which are partly based on [32]–[34]. For the scenario 2025 moreover, all nuclear power plants are phased out in favor of four additional combined cycle gas turbines (580 MW, 590 MW, 610 MW, 620 MW), reducing the number of plants from 228 to 223.

The production costs of a power plant are derived from its efficiency and fuel cost (Table I). The columns η_{2014}^{\max} and η_{1959}^{\max} detail the efficiencies at maximal load P_i^{\max} for units built in 2014 and 1959. The maximal efficiency η_i^{\max} of units constructed in-between these two years is assumed to increase linearly, and is interpolated using their commissioning year y_i ,

$$\eta_i^{\max} = (y_i - 1959) \frac{\eta_{2014}^{\max} - \eta_{1959}^{\max}}{2014 - 1959} + \eta_{1959}^{\max} \quad \forall i \in \mathcal{I}. \quad (31)$$

At minimal load P_i^{\min} , an efficiency of $\eta_i^{\min} = \eta_i^{\max} - \Delta\eta_i$ is assumed. Using the specific fuel cost C_{fuel} , the production costs at minimal and maximal production are defined as

$$C_{\text{fuel}} \frac{P_i^{\min}}{\eta_i^{\min}} \quad \text{and} \quad C_{\text{fuel}} \frac{P_i^{\max}}{\eta_i^{\max}}. \quad (32)$$

The production costs at intermediate production levels are interpolated affinely linear.

The coefficients of the start-up cost function in equation (7), the fixed start-up cost F_{rel} and the maximum variable start-up cost V_{rel} are given in Table I, both relative to the capacity of the respective unit. In addition, the table states the values assumed for the heat-loss coefficient λ as well as the specific fuel cost C_{fuel} .

In addition to power plant data, the model requires data of the residual load, i.e. of the difference between load and electricity production from must-run renewable power sources. The load data is taken from ENTSO-E [36], and scaled to a yearly electricity consumption of 520 TWh. Wind and solar

TABLE I
OVERVIEW OF INPUT DATA; VALUES FOR SU, SD ARE ASSUMED TO BE IDENTICAL TO P^{\min} . VALUES FOR RU AND RD ARE SET TO 1 AS THEY ARE ABOVE 2 %/MINUTE FOR ALL CONSIDERED TYPES OF POWER PLANTS [35].

| Type | # | P^{\min} [%] | η_{2014}^{\max} [%] | η_{1959}^{\max} [%] | $\Delta\eta$ [%] | V_{rel} [€/MW] | F_{rel} [€/MW] | λ | C_{fuel} [€/MWh _{th}] |
|---------|----|-------------------|-----------------------------|-----------------------------|---------------------|----------------------------|----------------------------|-----------|---|
| Nuclear | 9 | 60 | 37 | 37 | 2 | 120 | 80 | 0.03 | 3.60 |
| Lignite | 39 | 55 | 45 | 30 | 3 | 120 | 80 | 0.03 | 9.33 |
| Coal | 67 | 35 | 45 | 30 | 5 | 100 | 60 | 0.05 | 14.41 |
| CCGT | 36 | 50 | 60 | 45 | 7 | 60 | 40 | 0.1 | 22.00 |
| OCGT | 77 | 10 | 40 | 25 | 20 | 25 | 25 | 0.3 | 22.00 |

TABLE II
SCENARIOS FOR INSTALLED CAPACITIES OF RENEWABLE GENERATION

| Year | Wind On [GW] | Wind Off [GW] | PV [GW] | Biomass [GW] | Hydro [GW] |
|------|--------------|---------------|---------|--------------|------------|
| 2014 | 28 | 0.4 | 23 | 3 | 4 |
| 2025 | 40 | 10 | 50 | 5.5 | 4.5 |

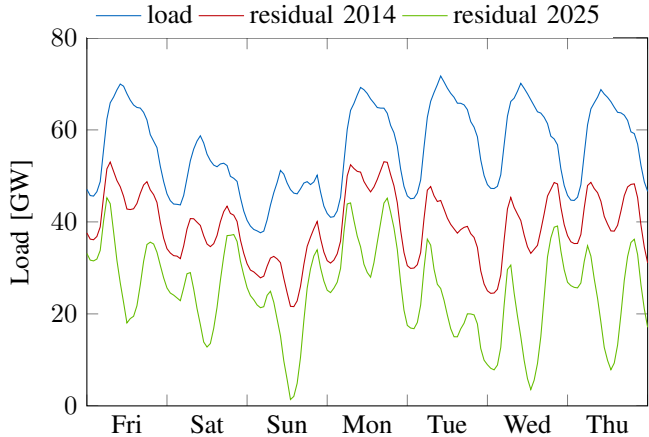


Fig. 3. Load and residual load for a sample week in 2014 and 2025, starting from the 4801th hour of the year.

electricity generation profiles are computed based on the NASA MERRA database [37] for the same base year. Afterwards, these profiles are scaled according to the respective installed capacity given in Table II. Biomass and hydro power plants are assumed to produce at full capacity.

Fig. 3 compares the full load and the residual load for an exemplary week in scenarios 2014 and 2025, starting on a Friday. The chosen week highlights the increased volatility of the residual load in future power systems. Furthermore, its first three days, on which the calculations in Section VII-E are based, comprise the three major types of days (workday, Saturday, and Sunday).

B. Compared Model Formulations

We evaluate our approach by comparing it to the state-of-the-art formulations introduced in Section II-B. The following models are considered in our numerical experiments:

- 1) 1-Bin: The model according to [8] with linear production costs and ramping constraints as described in inequalities (5-6). Minimum downtime and uptime is not considered. Different levels of start-up cost approximation tolerance K_{tol} are employed according to equation (14).
- 2) 1-Bin*: Same as 1-Bin, with the tightened start-up cost inequalities (13) instead of the original inequalities (8).
- 3) 3-Bin: Formulation of the start-up costs equivalent to P1 in [18]. Same as 1-Bin, except that start-up cost inequalities (8) are replaced by the inequalities (9-12).
- 4) Temp: New approach with explicit modeling of the power plant temperature, as described in Section V.
- 5) T-cuts: Same as Temp, with the additional residual temperature inequalities as presented in Section VI.

The numerical experiments are performed using two of the most often employed solvers and modeling frameworks—Xpress/Mosel and CPLEX/GAMS. As GAMS does not allow recursive functions, the cutting planes of the T-cut formulation are separated externally using Python [38].

C. Integrality Gap

An important criterion of a problem formulation is its integrality gap, which measures the influence of the integrality constraints on the optimal solution, and is defined as

$$\text{integrality gap} = \frac{\text{integral optimal value}}{\text{fractional optimal value}} - 1.$$

Smaller integrality gaps mean better lower bounds, which lead to faster solution times. The best possible integrality gap is 0, which would mean that the optimal objective value of the formulation does not depend on the integrality constraints.

Fig. 4 shows the integrality gap of the four models, taken over 14 time ranges of length $T = 72$, spread over different seasons of the year (first period $S \in \{1248k + 433 : k \in [0..13]\}$). It clearly illustrates the advantage of modeling the temperature as an explicit variable.

The median integrality gap of 1-Bin lies at 1.0239, and is slightly decreased to 1.0221 through the tightening in 1-Bin*. The 3-Bin model reduces the median integrality gap to around 1.0101, a reduction of 58% compared to 1-Bin, corresponding in magnitude to the results reported in [10]. The median integrality gap of the Temp formulation is 1.0085, which is cut down to 1.0021 in T-cuts; this is a reduction of 91% with respect to 1-Bin and of 79% with respect to 3-Bin.

In summary, Temp and T-cuts lead to significant reductions of the integrality gap, even with respect to the tighter formulation in [10], [15]. It should be mentioned that due to the simple base model, the integrality gaps in these numerical examples might be lower than in previously published papers. Still, the relative differences between the formulations will remain comparable in other settings.

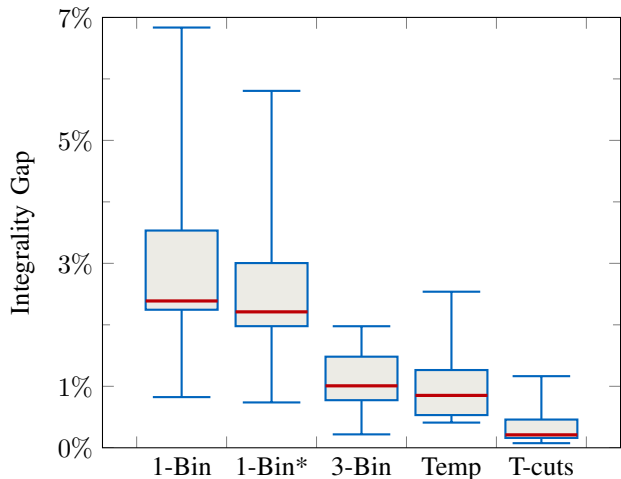


Fig. 4. Integrality gaps – 1 for 14 test cases with $T = 72$ periods. The temperature formulations outperform the step-wise formulations significantly. The impact of the RTIs shows when comparing Temp and T-cuts.

D. Computational Effort for Solving the LP

Another criterion for the quality of a formulation is the computational effort of solving its (initial) linear relaxation. To stay as close as possible to the practical application, especially with regard to the generation of the RTIs, we measured the solution time for the root node of the Branch&Cut tree. At the same time, we tried to remain close to the linear relaxation by disabling the integrality-specific algorithms of the solvers, i.e. presolve, integrated cuts, and heuristics (for tests with default settings, see Section VII-E).

Fig. 5 compares solution times of the linear relaxations for the same scenarios as in Fig. 4. The results clearly show that both temperature formulations considerably outperform 1-Bin, 1-Bin* and 3-Bin. Comparing Temp and T-cuts, we see that including the RTIs only leads to a moderate increase in computational effort.

The moderate increase from Temp to T-cuts indicates that including the RTIs does not increase the computational effort excessively.

E. Overall Computational Performance

After having shown improvements in two major criteria, the tightness (integrality gap) and the speed of the LP, we present results for the overall computational performance of our approach. Table III shows computation times for test cases of different sizes ($T \in \{24, 48, 72\}$ periods of one hour length) and different approximation tolerances K_{tol} . All test cases were started at $S = 4801$ (residual load is depicted in Fig. 3). Several observations can be made:

- Test cases in 2025 require more computational effort, due to the higher ratio of start-up to overall costs.
- 1-Bin and 1-Bin* fail to reach an optimality gap of 1% within 1 hour in 22% of the test cases. While 3-Bin solves all but 5% of the instances, both temperature formulations Temp and T-cuts never need more than 3 minutes to reduce the optimality gap to at most 1%.
- Temp and T-cuts reliably outperform the step-wise models with zero approximation tolerance ($K_{\text{tol}} = 0\%$).
- The performance of CPLEX and Xpress differs only slightly. For 1-Bin and 1-Bin*, Xpress tends to be slightly faster, whereas for 3-Bin it is the other way around.
- The distribution of the computation times of 1-Bin, 1-Bin* and 3-Bin is highly irregular. Of the test cases which were solved to an optimality gap of 1% in 1 hour, 90% were solved in less than 8 minutes. This may stem from the typical behavior of Mixed Integer Problems, where the optimality gap improves very slowly once the solution process enters the Branch&Bound tree. Fig. 6 exemplifies the convergence behavior for an instance of scenario 2025 with $T = 72$.

Table IV shows the remaining optimality gap after a solution time of 15 minutes. In several instances, the CPLEX solver did not finish the initial linear relaxation, therefore no optimality gap was calculated. Some additional characteristics are observed:

- The optimality gap quality of the solution is quite similar for Xpress and CPLEX for 1-Bin and 1-Bin*.

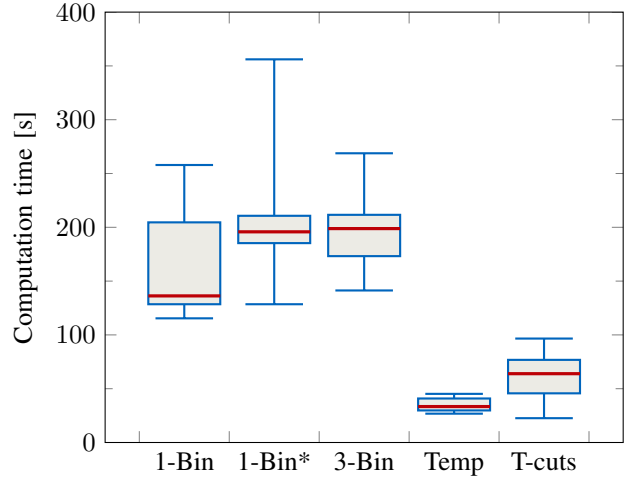


Fig. 5. Solution times of the linear relaxation for 14 test cases with $T = 72$ periods. Temp is considerably faster than the step-wise formulations, and the additional RTIs in T-cuts do not increase the computational effort excessively.

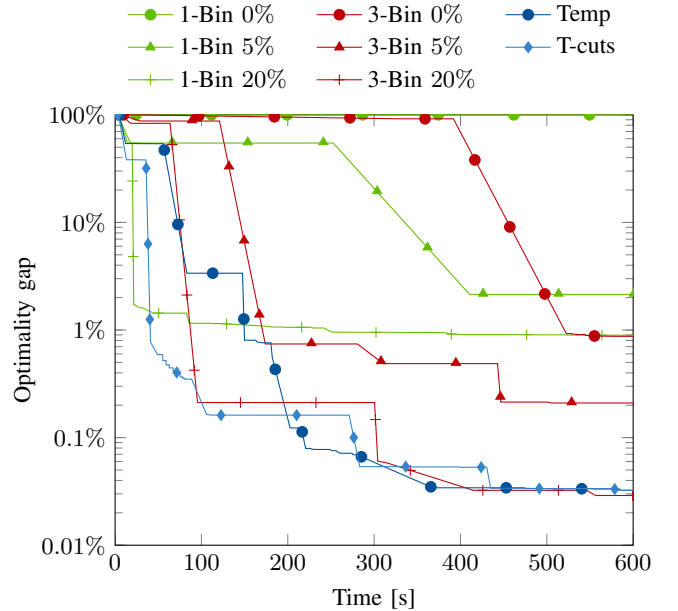


Fig. 6. Convergence of the optimality gap for an instance with 72 periods. The percentages in the legend represent start-up cost approximation tolerances K_{tol} .

- Again, the performance of CPLEX is better for the 3-Bin formulation, whereas for Xpress it is the other way around.

F. Performance With Scaling to a Larger Number of Periods

An essential aspect in computational efficiency is the behavior with model scaling. Especially scaling to a higher number of modeled periods seems highly relevant for future operational planning for two reasons:

- 1) As the residual load will become more volatile it will be beneficial to increase the time resolution [39].
- 2) As renewable generation changes over several days and weeks, the storage management requires to consider longer time horizons than today where it is mainly driven by day and night variation of load.

TABLE III
COMPARISON OF COMPUTATIONAL PERFORMANCE—CONVERGENCE TIME [S] TO A MIP-GAP OF 1%

| Scenario | 1-Bin | | | 1-Bin* | | | 3-Bin | | | Temp T-cuts | |
|-------------------|------------------|-------|--------|--------|-------|--------|--------|-------|-------|-------------|-------|
| | K_{tol} | 0% | 5% | 20% | 0% | 5% | 20% | 0% | 5% | 20% | x |
| 2014, 24h, CPLEX | 6.6 | 2.7 | 1.8 | 53.9 | 3.1 | 1.7 | 7.3 | 4.0 | 3.6 | 2.8 | 2.8 |
| 2014, 48h, CPLEX | 951.6 | 11.7 | 6.8 | 458.6 | 12.0 | 6.7 | 86.8 | 15.3 | 12.7 | 85.5 | 13.0 |
| 2014, 72h, CPLEX | >1h | 54.5 | 21.7 | >1h | 54.4 | 15.7 | 712.4 | 226.0 | 66.4 | 261.9 | 36.6 |
| 2014, 24h, Xpress | 5.2 | 1.2 | 1.2 | 4.4 | 1.6 | 1.1 | 5.3 | 2.8 | 1.7 | 1.8 | 1.9 |
| 2014, 48h, Xpress | 31.8 | 3.6 | 3.6 | 42.3 | 5.9 | 3.4 | 125.0 | 58.21 | 26.3 | 43.9 | 44.1 |
| 2014, 72h, Xpress | 218.8 | 15.6 | 15.5 | 225.0 | 26.7 | 15.5 | 3303.7 | 970.8 | 201.7 | 114.1 | 114.1 |
| 2025, 24h, CPLEX | 8.4 | 3.7 | 1.9 | 60.6 | 5.8 | 1.7 | 7.2 | 3.9 | 3.6 | 4.4 | 2.6 |
| 2025, 48h, CPLEX | >1h | 482.6 | 81.4 | >1h | 991.6 | 10.6 | 300.6 | 105.9 | 39.8 | 29.3 | 19.8 |
| 2025, 72h, CPLEX | >1h | >1h | 246.34 | >1h | >1h | 103.9 | 441.6 | 175.3 | 87.8 | 150.2 | 41.4 |
| 2025, 24h, Xpress | 6.7 | 1.2 | 1.2 | 6.4 | 2.8 | 1.1 | 5.2 | 2.9 | 3.0 | 4.3 | 4.3 |
| 2025, 48h, Xpress | >1h | 10.5 | 10.5 | >1h | >1h | 9.2 | 1746.1 | 68.9 | 50.4 | 31.6 | 31.8 |
| 2025, 72h, Xpress | >1h | >1h | >1h | >1h | >1h | 1075.4 | >1h | >1h | 135.9 | 117.1 | 116.7 |

TABLE IV
COMPARISON OF COMPUTATIONAL PERFORMANCE—OPTIMALITY GAP IN % AFTER A CALCULATION TIME OF 15 MIN

| Scenario | 1-Bin | | | 1-Bin* | | | 3-Bin | | | Temp T-cuts | |
|-------------------|------------------|-------|-------|--------|-------|-------|-------|-------|-------|-------------|-------|
| | K_{tol} | 0% | 5% | 20% | 0% | 5% | 20% | 0% | 5% | 20% | x |
| 2014, 24h, CPLEX | 0.001 | 0.000 | 0.000 | 0.004 | 0.000 | 0.000 | 0.000 | 0.000 | 0.000 | 0.001 | 0.008 |
| 2014, 48h, CPLEX | - | 0.209 | 0.146 | 0.314 | 0.203 | 0.112 | 0.010 | 0.007 | 0.004 | 0.014 | 0.018 |
| 2014, 72h, CPLEX | - | 0.739 | 0.404 | - | 0.613 | 0.383 | 0.780 | 0.026 | 0.005 | 0.037 | 0.043 |
| 2014, 24h, Xpress | 0.000 | 0.000 | 0.000 | 0.000 | 0.000 | 0.000 | 0.000 | 0.000 | 0.000 | 0.000 | 0.000 |
| 2014, 48h, Xpress | 0.415 | 0.199 | 0.199 | 0.297 | 0.244 | 0.189 | 0.370 | 0.151 | 0.015 | 0.017 | 0.012 |
| 2014, 72h, Xpress | 0.863 | 0.434 | 0.434 | 0.874 | 0.758 | 0.445 | 1.540 | 1.237 | 0.383 | 0.049 | 0.032 |
| 2025, 24h, CPLEX | 0.084 | 0.052 | 0.003 | 0.047 | 0.006 | 0.002 | 0.000 | 0.000 | 0.000 | 0.000 | 0.000 |
| 2025, 48h, CPLEX | 53.883 | 0.972 | 0.491 | 1.433 | 1.037 | 0.382 | 0.095 | 0.080 | 0.008 | 0.011 | 0.013 |
| 2025, 72h, CPLEX | - | 1.776 | 0.866 | - | 1.629 | 0.730 | 0.873 | 0.067 | 0.020 | 0.018 | 0.023 |
| 2025, 24h, Xpress | 0.072 | 0.009 | 0.009 | 0.077 | 0.062 | 0.005 | 0.000 | 0.000 | 0.000 | 0.000 | 0.000 |
| 2025, 48h, Xpress | 1.305 | 0.615 | 0.615 | 1.140 | 1.053 | 0.487 | 1.584 | 0.224 | 0.091 | 0.057 | 0.028 |
| 2025, 72h, Xpress | 2.168 | 1.192 | 1.192 | 2.162 | 1.958 | 1.191 | 3.055 | 3.614 | 0.458 | 0.082 | 0.060 |

Fig. 7 visualizes the scaling behaviour of all formulations, with approximation tolerances $K_{\text{tol}} \in \{0\%, 5\%, 20\%\}$. The number of periods of the modeled instances varies from $T = 24$ to $T = 360$, while the remaining parameters correspond to the instances used to analyze the integrality gap in Subsection VII-C. The first chart shows the number of instances which have been solved to an optimality gap of 1% within 1 hour of computation time. The second chart exhibits the average solution times of each formulation for all T with at least two instances solved.

1-Bin and 1-Bin* either solve instances relatively quickly, or fail to reach the 1% optimality gap within 1 hour due to their convergence behavior (see Fig. 6). A slight advantage is discernible for 1-Bin*.

Both in terms of solved instances and mean solution time, 3-Bin dominates 1-Bin and 1-Bin*, and does not show the same abrupt increase in computational time for a higher number of periods. For $K_{\text{tol}} = 20\%$, its computation times rival those of Temp, albeit Temp consistently solves more instances.

Finally, the strong impact of the RTIs becomes apparent when comparing Temp and T-cuts for a higher number of periods.

VIII. CONCLUSION

We have improved the modeling of start-up costs in Unit Commitment models for both the commonly used exponential start-up cost function (Definition (7)) and for arbitrary, increasing start-up cost functions.

For general increasing start-up cost functions, we have shown that the inequalities used by the state-of-the-art formulations can be tightened. For exponential start-up cost functions, we have presented the temperature formulation, which accurately models the start-up costs while considerably outperforming the state-of-the-art formulation—even with high approximation tolerances. The increased performance may be attributed to both the faster LP relaxation and the typically smaller integrality gap.

Moreover, we have introduced cutting planes for this temperature formulation, which can be separated at a small computational cost. Using these cuts, the integrality gap can be reduced significantly, leading to even better solution times, especially for relatively large instances.

As noted, if there are no hard constraints on the operational states, it can be proved that the integrality gap can not be further reduced by cuts which act solely on the start-up cost and operational state variables of a single unit. This suggests a

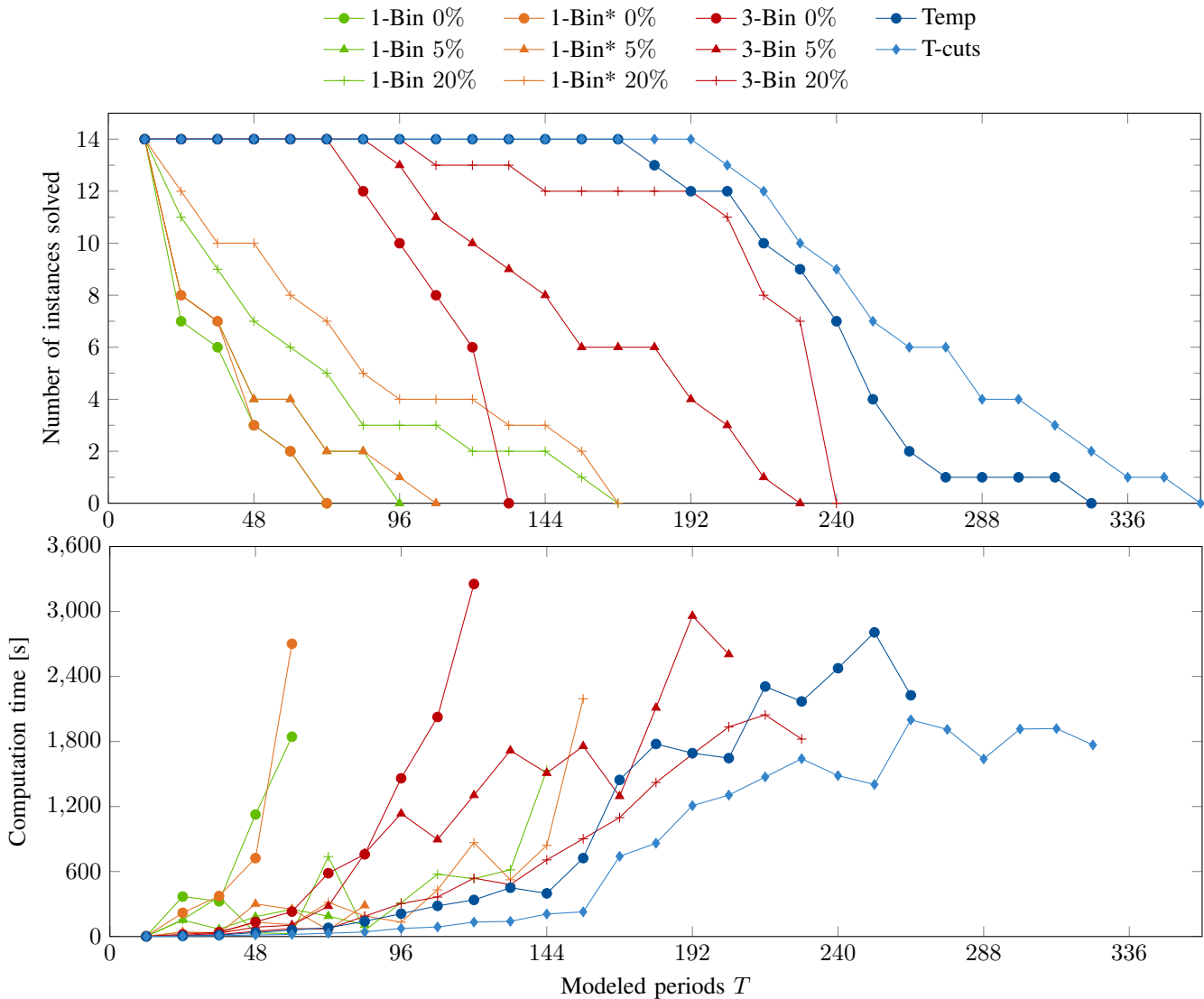


Fig. 7. Scaling of computational effort with problem size for all formulations and different approximation tolerances K_{tol} . The first chart shows the number of instances solved to an optimality gap of 1% within 1 hour of computation time. The second chart details the average solution time of each formulation for all modeled periods T with at least two solved instances.

very challenging question for future research: How to separate cuts which use variables from multiple units viable? To the best of our knowledge, such cuts have not been considered yet, except for knapsack cuts regarding the maximal capacity of each unit and the residual load.

Our numerical results show that, when using state-of-the-art step-wise start-up cost formulations, one always has to strike a compromise between fast linear relaxations and low approximation errors. It seems viable to solve this dilemma by separating constraints (8) and (13) in a cutting plane algorithm. While we do not expect such an approach to outperform the temperature formulation, it could be applied to units with start-up cost functions which do not correspond to (7).

Finally, we hope that the novel temperature formulation with its simple physical interpretation will inspire and facilitate fundamental future extensions of the Unit Commitment problem.

REFERENCES

- [1] International Energy Agency, *World Energy Outlook 2013*. Organization for Economic Co-operation and Development (OECD), 2013.
- [2] P. Keatley, A. Shibli, and N. J. Hewitt, "Estimating power plant start costs in cyclic operation," *Applied Energy*, vol. 111, pp. 550–557, Nov. 2013.
- [3] M. Huber, T. Hamacher, C. Ziemer, and H. Weber, "Combining LP and MIP approaches to model the impacts of renewable energy generation on individual thermal power plant operation," in *2013 IEEE Power and Energy Society General Meeting (PES)*, Jul. 2013, pp. 1–5.
- [4] R. Baldick, "The generalized unit commitment problem," *IEEE Trans. Power Syst.*, vol. 10, no. 1, p. 465–475, Feb. 1995.
- [5] T. Hughes, *Networks of Power: Electrification in Western Society, 1880–1930*, 2nd ed. Baltimore: Johns Hopkins University Press, 1993.
- [6] G. Sheble and G. Fahd, "Unit commitment literature synopsis," *IEEE Trans. Power Syst.*, vol. 9, no. 1, pp. 128–135, Feb. 1994.
- [7] N. Padhy, "Unit commitment—a bibliographical survey," *IEEE Trans. Power Syst.*, vol. 19, no. 2, pp. 1196–1205, May 2004.
- [8] M. Carrión and J. Arroyo, "A computationally efficient mixed-integer linear formulation for the thermal unit commitment problem," *IEEE Trans. Power Syst.*, vol. 21, no. 3, pp. 1371–1378, Aug. 2006.
- [9] C. Simoglou, P. Biskas, and A. Bakirtzis, "Optimal self-scheduling of a thermal producer in short-term electricity markets by MILP," *IEEE Trans. Power Syst.*, vol. 25, no. 4, pp. 1965–1977, Nov. 2010.

- [10] G. Morales-España, J. Latorre, and A. Ramos, "Tight and compact MILP formulation for the thermal unit commitment problem," *IEEE Trans. Power Syst.*, vol. 28, no. 4, pp. 4897–4908, Nov. 2013.
- [11] J. Lee, J. Leung, and F. Margot, "Min-up/min-down polytopes," *Discrete Optimization*, vol. 1, no. 1, pp. 77–85, Jun. 2004.
- [12] D. Rajan and S. Takriti, "Minimum up/down polytopes of the unit commitment problem with start-up costs," *IBM Research Division*, Jun. 2005. [Online]. Available: <http://www.research.ibm.com/people/d/dpkrijn/DeepakTR.pdf>
- [13] A. Frangioni, C. Gentile, and F. Lacalandra, "Tighter approximated MILP formulations for unit commitment problems," *IEEE Trans. Power Syst.*, vol. 24, no. 1, pp. 105–113, Feb. 2009.
- [14] A. Viana and J. P. Pedroso, "A new MILP-based approach for unit commitment in power production planning," *International Journal of Electrical Power & Energy Systems*, vol. 44, no. 1, pp. 997–1005, Jan. 2013.
- [15] J. Ostrowski, M. Anjos, and A. Vannelli, "Tight mixed integer linear programming formulations for the unit commitment problem," *IEEE Trans. Power Syst.*, vol. 27, no. 1, pp. 39–46, Feb. 2012.
- [16] M. P. Nowak and W. Römisch, "Stochastic lagrangian relaxation applied to power scheduling in a hydro-thermal system under uncertainty," *Annals of Operations Research*, vol. 100, no. 1–4, pp. 251–272, Dec. 2000.
- [17] R. Brandenberg and M. Silbernagl, "Implementing a unit commitment power market model in FICO Xpress-Mosel," FICO Xpress Optimization Suite whitepaper, FICO, 2014.
- [18] G. Morales-España, J. Latorre, and A. Ramos, "Tight and compact MILP formulation of start-up and shut-down ramping in unit commitment," *IEEE Trans. Power Syst.*, vol. 28, no. 2, pp. 1288–1296, May 2013.
- [19] J. P. Pedroso, M. Kubo, and A. Viana, "Unit commitment with valve-point loading effect," *arXiv:1404.4944 [cs, math]*, Apr. 2014. [Online]. Available: <http://arxiv.org/abs/1404.4944>
- [20] C. Hernandez-Aramburo, T. Green, and N. Mugniot, "Fuel consumption minimization of a microgrid," *IEEE Trans. Ind. Appl.*, vol. 41, no. 3, pp. 673–681, May 2005.
- [21] A. Wood and B. Wollenberg, *Power generation, operation and control*, 2nd ed. Wiley, 1996.
- [22] H. Spliethoff, *Power Generation from Solid Fuels*, ser. Power Systems. Springer Berlin Heidelberg, 2010.
- [23] L. Garver, "Power generation scheduling by integer programming-development of theory," *AIEE Trans. Power App. Syst., Part III*, vol. 81, no. 3, pp. 730–734, Apr. 1962.
- [24] J. Muckstadt and R. Wilson, "An application of mixed-integer programming duality to scheduling thermal generating systems," *IEEE Trans. Power App. Syst.*, vol. PAS-87, no. 12, pp. 1968–1978, Dec. 1968.
- [25] D. Streiffert, R. Philbrick, and A. Ott, "A mixed integer programming solution for market clearing and reliability analysis," in *2005 IEEE Power Engineering Society General Meeting*, Jun. 2005, pp. 2724–2731 Vol. 3.
- [26] R. Brandenberg, M. Huber, and M. Silbernagl, "Modeling the summed start-up cost in mip unit commitment via power plant temperatures," in preparation.
- [27] M. R. Bussieck, "Introduction to GAMS branch-and-cut facility," GAMS Development Corp., Technical report, 2003. [Online]. Available: <http://www.gams.com/docs/bch.htm>
- [28] "FICO Xpress-Optimizer reference manual," 2014.
- [29] J. Vuillemin, "A unifying look at data structures," *Communications of the ACM*, vol. 23, no. 4, pp. 229–239, Apr. 1980.
- [30] H. N. Gabow, J. L. Bentley, and R. E. Tarjan, "Scaling and related techniques for geometry problems," in *Proceedings of the Sixteenth Annual ACM Symposium on Theory of Computing*, ser. STOC '84. New York, NY, USA: ACM, 1984, p. 135143.
- [31] Bundesnetzagentur, "List of power plants," Apr. 2014. [Online]. Available: <http://www.bnetza.de>
- [32] N. Kumar, P. M. Besuner, S. A. Lefton, D. D. Agan, and D. A. Hileman, "Power plant cycling costs," Intertek APTECH, Sunnyvale, California, Tech. Rep., Apr. 2012, research Report, prepared for National Renewable Energy Laboratory and Western Electricity Coordinating Council.
- [33] EURELECTRIC, "Efficiency in electricity generation," EURELECTRIC, Brussels, Belgium, Tech. Rep., Jul. 2013.
- [34] J. Egerer, C. Gerbaulet, R. Ihlenburg, F. Kunz, B. Reinhard, C. v. Hirschhausen, A. Weber, and J. Weibezahn, "Electricity sector data for policy-relevant modeling: Data documentation and applications to the german and european electricity markets," Deutsches Institut für Wirtschaftsforschung (DIW), Berlin, Data Documentation 72, 2014.
- [35] A. Schröder, F. Kunz, J. Meiss, R. Mendelevitch, and C. Hirschhausen, von, "Current and prospective costs of electricity generation until 2050 - data documentation," Deutsches Institut für Wirtschaftsforschung (DIW), Berlin, Data Documentation 68, Jul. 2013.
- [36] ENTSO-E, European Network of Transmission System Operators for Electricity, "Hourly load values," Tech. Rep., 2007. [Online]. Available: <http://www.entsoe.eu/data/data-portal/consumption/>
- [37] M. M. Rienecker *et al.*, "MERRA: NASA's modern-era retrospective analysis for research and applications," *Journal of Climate*, vol. 24, no. 14, pp. 3624–3648, Jul. 2011.
- [38] GAMS Development Corp., "Gams python api documentation version 24.2," Technical report, 2014. [Online]. Available: http://www.gams.com/dd/docs/api/GAMS_python.pdf
- [39] J. P. Deane, G. Drayton, and B. P. Ó Gallachóir, "The impact of sub-hourly modelling in power systems with significant levels of renewable generation," *Applied Energy*, vol. 113, pp. 152–158, Jan. 2014.



Matthias Silbernagl received his Dipl.-Math. (M.Sc. in Mathematics) from the Technische Universität München (TUM), Germany, in 2009. Currently, he is a doctoral candidate at the Chair for Applied Geometry and Discrete Mathematics at TUM. As an IGSSSE associate, he participates in the interdisciplinary project "Integration of Renewables".

His area of research includes Mixed Integer Programming and Polyhedral Studies, with a focus on the family of Unit Commitment problems.



Matthias Huber received his Dipl.-Ing. (M.Sc.) in Mechanical Engineering from Technische Universität München (TUM) and his B.Sc. in Economics from Ludwig Maximilians Universität (LMU), both in 2010. He is now pursuing his PhD at the Institute for Renewable and Sustainable Energy Systems at TUM. His research interests include optimal planning, operation, and economics of power systems.



René Brandenberg received his Dipl.-Math. from Universität Trier in 1998 and his Dr. rer. nat. (Ph.D.) from TUM in 2003. He is now on a permanent position at the Chair for Applied Geometry and Discrete Mathematics at TUM and his main research areas are convex and computational geometry as well as their application in optimization.